

TEVATRON RESULTS ON THE STANDARD MODEL HIGGS SEARCH IN THE HIGH MASS REGION

Richard St. Denis

*University of Glasgow – Department of Physics and Astronomy
Glasgow G12 8QQ – United Kingdom*



The latest results for the Tevatron search for the Higgs boson decaying to W boson pairs in proton antiproton collisions at $\sqrt{s} = 1960$ GeV/c² are presented. The combined Tevatron results exclude a Standard Model Higgs at 95% confidence level for a higgs mass M_H in the range $162 \leq M_H \leq 166$ GeV/c². Further progress shows that each experiment should have sensitivity to the Standard Model Higgs with the existing dataset and that final Tevatron results for the decay of Higgs to WW will be sensitive to Higgs masses in or exceeding the range $146 \leq M_H \leq 183$ GeV/c².

1 Introduction

The Tevatron experiments have enjoyed an annual doubling of the integrated luminosity delivered and recorded. This has led to an avalanche of new results in the area of electroweak symmetry breaking and in particular in direct searches for the Higgs. The physics reach of the Tevatron is built on a mountain of measurements that confirm the ability of the Tevatron collaborations to use their detectors to find new particles. Each measurement is of itself a significant result. Measurements begin with the largest cross section processes, those of B physics, but move on to processes with small branching ratios and backgrounds that are hard to distinguish from the signal. The measurement of B_s oscillations¹ demonstrates the performance of the silicon tracking and vertexing. Discovery of single top production², WZ production³, and evidence for the ZZ production⁴ in both leptonic and now hadronic modes⁵ provide the final base camp from which the Higgs summit is in sight. Multivariate techniques in the Higgs analysis are at the heart of what is required to reach sensitivity to the Higgs. Processes such as single top and ZZ act as important messengers heralding the impending arrival of the Higgs. This journey through lower and lower cross section processes represents our approach to provide convincing evidence of these processes, first as discovery then as measurements that constrain the Standard Model.

2 Direct Searches for the Standard Model Higgs

The Higgs searches at the Tevatron are separated into “high” and “low” mass channels. The high mass channel is characterized by the decay mode $H^0 \rightarrow W^+W^-$ whereas the low mass channels focus on decays to b quark-antiquark pairs or tau pairs.

There are four main production mechanisms for the Standard Model Higgs at the Tevatron: gluon fusion, $gg \rightarrow H^0$, associated production or “Higgsstrahlung”, $q\bar{q} \rightarrow (W^\pm/Z^0)H^0$, and vector boson fusion (VBF), $q\bar{q} \rightarrow W(Z)q'W(Z)\bar{q}' \rightarrow H^0q'\bar{q}'$. In all cases the high mass Higgs search uses the decay modes into charged leptons and neutrinos: $H^0 \rightarrow W^+W^- \rightarrow \ell^+\ell^-\bar{\nu}_\ell+\nu_\ell$. The charged leptons ℓ may be electrons, muons or taus. In the case of taus current searches include the τ decay channels $\tau^- \rightarrow e^-\bar{\nu}_e$ or $\tau^- \rightarrow \mu^-\bar{\nu}_\mu$ and charge conjugate channels. New results for hadronic decays of the τ from one W where the other W decays to an electron or muon are reported here.

The search for the decay of Higgs to W boson pairs which decay to leptons has sensitivity that is comparable to the low mass modes down to a Higgs mass of about $M_h = 120$ to 130 GeV/c^2 and reach above 170 GeV/c^2 with the best sensitivity around $M_h = 2M_w$, where M_w is the W boson mass. The high mass mode is characterized by two high transverse momentum oppositely charged leptons which have a spin correlation that leads to angular correlations between the charged leptons that distinguish it from other Standard Model modes of charged dilepton production. Requiring that the charged leptons be isolated removes the large number of charged dileptons from B decays as evidenced by the fact that the kinematics of the remaining dilepton events are well described by the Drell-Yan predictions. Drell-Yan production is the dominant source of oppositely charged lepton pairs at the Tevatron. These leptons tend to have an azimuthal separation of 180 degrees and these events are easily distinguished from Higgs events because they have no missing transverse energy. Once a transverse energy cut is applied, the background composition depends on the number of jets and the invariant mass of the leptons, $M_{\ell\ell}$. A majority of events are examined with the requirement that $M_{\ell\ell} > 16(15)$ GeV/c^2 CDF (D0). Events with 0 jets are dominated by WW background while those with 1 jet have a background consisting of a mixture of Drell Yan and WW. Events with two more jets sample are dominated by top quarks. CDF explicitly separates the analyses by jet number whereas D0 uses the number of jets as input to the multivariate analyses described below but does a separate analysis for each dilepton type. CDF also does an analysis of $M_{\ell\ell} < 16$ GeV/c^2 where the dominant background is $W\gamma$ production. The charged leptons in the WW background tend not to have the strong azimuthal correlation offered by the Higgs decay. Other differences in kinematic variables between the background and signal are exploited by using the multivariate techniques described in the next section. Results for the high mass Higgs are shown for the D0 analysis in Fig. 1 for $H^0 \rightarrow W^+W^- \rightarrow \mu^-e^+\bar{\nu}_\mu\nu_e$ and complex conjugate modes.

3 Multivariate Techniques

The major multivariate techniques in use are the Matrix Element (ME) and the Neural Net (NN). These are compared and contrasted here.

The ME method employs leading order computations of the matrix elements for the signals and backgrounds. The inputs are the measured four-vectors of the leptons and jets and the x- and y-components of the missing transverse energy. The probability that these values represent each physics process is computed by integrating over the matrix element while convolving the matrix element quantities with a *transfer function* that converts them to values that are observable. This transfer function represents the detector resolution and may include initial state radiation effects. A likelihood discriminator is formed by taking the ratio of the probability that the observed quantities represent the signal, divided by the total probability that the event is signal

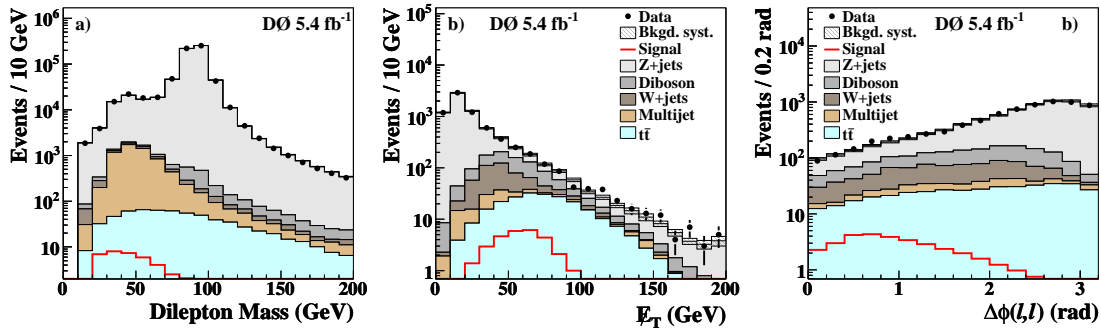


Figure 1: The invariant mass of isolated dileptons(left), the E_T spectrum of isolated leptons (center) and the cosine of the angle between dileptons after cuts for input to the discriminant analysis for the D0 experiment.

plus the probabilities that the event is background. The background probabilities are weighted according to their relative abundances. The computation of these probabilities is carried out on a set of simulated background and signal events. The distribution of the ME computation for each background and the signal is used to form a *template*.

At this point the analysis proceeds as for any cut analysis, with the likelihood ratio being used in place of a kinematic quantity such as the angular separation of the charged leptons. The data distribution is computed and the data are fitted to the templates with the signal normalization allowed to vary freely and the background normalizations constrained within the estimated systematic uncertainties. The probability that the background represents the data compared to the probability that the background plus the signal represents the data is evaluated by performing a number of pseudoexperiments on the background alone to represent the statistical accuracy of the data in the absence of a signal, and the distribution of the cross sections is formed. This distribution is compared to the fit result for the actual data and the probability that the data are consistent with background is computed by determining the number of pseudoexperiments that have a value less than or equal to that observed. If the data lie within 95% of the experiments performed, a limit is set. If the data exceed expectations then a cross section can be determined.

The NN approach contains similar elements to that of the ME. First there is a matrix element computation performed in both followed by a conversion of values from the ideal four vectors to the observed quantities. These values are sampled over some region of phase space. In the case of the ME, the phase space is spanned using a program that performs a numerical integral over that space whereas in the NN, simulated events that are meant to span a sufficient portion of the phase space are generated and the minimization of the NN determines the overall response. Each has limitations in numerical methods of the integration and in the representation of the response of the detector. Either of the methods can be computationally intensive.

The two approaches also contain complementary characteristics. While the four vectors that are input to the ME are easy to identify, the functional form that characterizes the physics is not obvious. This becomes important in understanding how to determine the systematic uncertainties. For example, the Higgs to WW decay mode must depend on the angle of the leptons and hence it is important to determine how well the detector measures these angles. For the NN it is less obvious what values to choose and one must make a guess at what will be the important variables. Simply giving the same four vectors that were input to the ME may fail to work well if the statistics for populating the phase space is poor and variables that are not helpful in discriminating are examined by the NN. However, the most sensitive variables can be determined and the systematic uncertainties are evaluated by a straightforward variation of the most important discriminator and examination of the change of the output distribution.

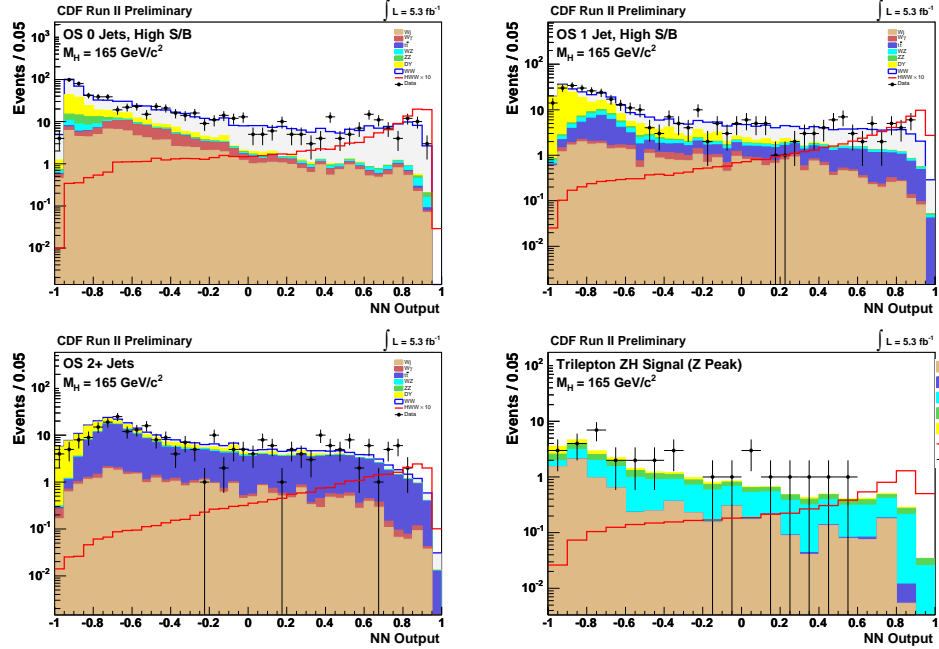


Figure 2: The Neural Net score distribution for opposite sign dileptons in the 0, 1 and 2 jet channels and for trileptons where an opposite sign pair invariant masses are in a 10 GeV window around the Z mass.

The differences in the approaches can be exploited to help determine the quantities that are important in the ME computation while at the same time providing evidence that the quantities needed in the NN computation have been included. This is accomplished by including the ME computation as input to the NN. If this shows significant improvement, then important values have been missed in the NN inputs. If there is little change, then values can be removed from the input list of the NN until a change is noticed, or conversely, they can be added one at a time. This shows which quantities are most important in the ME.

3.1 Control Regions

Control regions play an important role in the quantitative computation of backgrounds and their systematic uncertainties and in determining that the lepton identification is properly done. For example in the $H^0 \rightarrow W^+W^- \rightarrow (e)\mu^+\tau^+\bar{\nu}_{(e)\mu}\nu_\tau$ where the τ decays hadronically, requiring the invariant mass of the τ and $(e)\mu$ to be larger than $20 \text{ GeV}/c^2$, $E_T < 20 \text{ GeV}/c^2$ and the azimuthal separation of the $(e)\mu$ and the missing transverse energy to be less than 0.5 leads to a very pure sample of $Z \rightarrow \tau^+\tau^-$ decays in which the tau properties may be examined and systematic uncertainties in the difference between the simulation and data can be determined.

3.2 Channels with Smaller Contributions

Associated production with $H^0 \rightarrow W^+W^-$ leads to events with two charged leptons having the same sign, or to trilepton events. While the yields of these are much lower than of gluon fusion, the background compositions are very different: there is very little background. No channel is left behind because if an excess begins to emerge in one of the larger channels, one expects to see a small number of events in these channels with very little background. These also contribute to the overall sensitivity of the analysis. The main background to these analyses is WZ production.

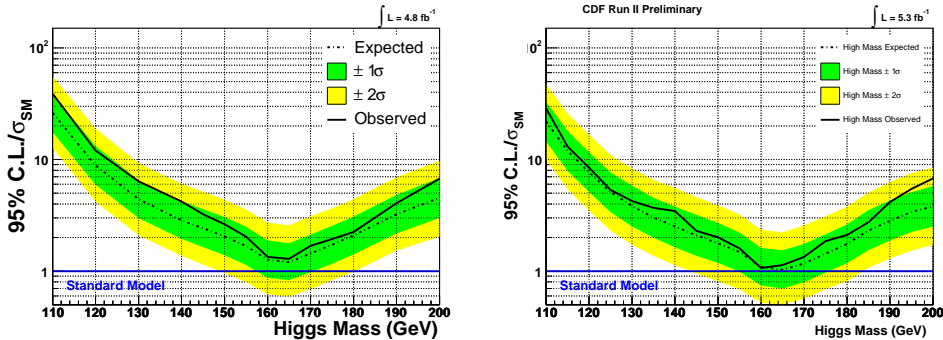


Figure 3: 95% confidence limits on the Standard Model Higgs boson for various masses for CDF with an integrated luminosity of 4.8 (left) and 5.4 fb^{-1} along with improvements described in the text.

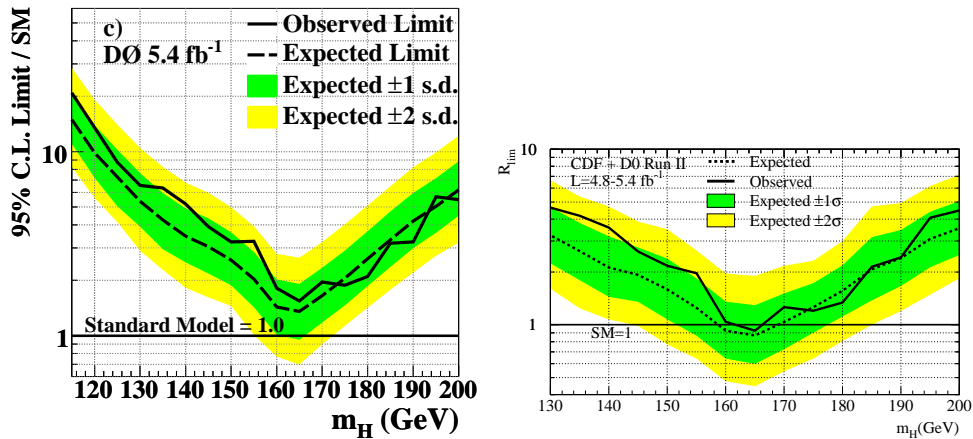


Figure 4: 95% confidence limits on the Standard Model Higgs boson for various masses for D0(left) and combined with the CDF 4.8 fb^{-1} analysis.

3.3 Results

Representative results for the neural net analysis are shown in Figure 2 before the fit is performed. The data having low neural net score values provide a strong control over the background and its dynamics as reflected in the neural net. The contribution of a Higgs signal is fit simultaneously with variation of the backgrounds within their uncertainties but as constrained by the NN distribution. It is also noteworthy that for $M_H = 165\text{GeV}/c^2$ the two experiments expect of order 70 Standard Model Higgs events.

3.4 Limits

As described in Section 3 a fit to the cross section for a particle having the dynamics of a Standard Model Higgs is performed on the NN distributions. This is done separately for each experiment^{6 7} and then combined⁸ where the handling of systematic uncertainties is described in the references. The CDF results using 4.8 fb^{-1} of integrated luminosity are shown in Figure 3, the D0 results and the combined CDF and D0 results are shown in Figure 4. The sensitivity to the Standard Model Higgs cross section covers the range $159 \leq M_H \leq 169 \text{ GeV}/c^2$ with an observed 95% exclusion probability in the range $162 \leq M_H \leq 166 \text{ GeV}/c^2$.

3.5 Outlook

The Tevatron is expected to double its data sample and additional improvements over the reported limits are available. CDF has increased the sample size from having an average integrated luminosity of 4.8 fb^{-1} to 5.3 fb^{-1} giving about a 5% improvement in sensitivity. But more importantly, the additional trilepton mode, the sample with $M_{\ell\ell} < 16 \text{ GeV}/c^2$, including VH and VBF for the 0 jet analysis and optimization of the electron selection leads to a 15% improvement in sensitivity as shown in Figure 3. The expected sensitivity at $M_H = 165 \text{ GeV}/c^2$ is now 1.03 times the Standard Model. If one then takes these improvements and assumes D0 achieves similar results, the sensitivity improves from covering the range $159 \leq M_H \leq 169 \text{ GeV}/c^2$ just reported to $156 \leq M_H \leq 174 \text{ GeV}/c^2$. With the expected doubling of the data by the end of 2011 the sensitivity extends to $146 \leq M_H \leq 183 \text{ GeV}/c^2$ and with further improvements in the methods, this could cover $136 \leq M_H \leq 190 \text{ GeV}/c^2$.

4 Conclusions

This conference is held at a remarkable moment in the understanding of electroweak symmetry breaking. Rapid changes in data collection and more sophisticated experimental technique are leading to a constantly changing picture. The Tevatron has delivered more than 8 fb^{-1} and has recently improved its luminosity by another 20%. Evidence and discovery of channels in WZ, ZZ and single top, the messengers of the Higgs, have now been observed. Of particular note is the observation of the hadronic modes of the W/Z in the WW and ZZ production. The strategy of “no channel too small” has been successful, lending additional sensitivity and a different background composition. The sensitivity of the combined Tevatron experimental result to the Standard Model Higgs cross section covers the range $159 \leq M_H \leq 169 \text{ GeV}/c^2$ with an observed 95% exclusion probability in the range $162 \leq M_H \leq 166 \text{ GeV}/c^2$. Based only on collecting more data, the sensitivity extends to $146 \leq M_H \leq 183 \text{ GeV}/c^2$ and with further improvements in the methods, this goes to $136 \leq M_H \leq 190 \text{ GeV}/c^2$.

5 Acknowledgments

The author would like to thank the organizers for this invitation to speak and the wonderful atmosphere of the conference.

References

1. A. Abulencia *et al*, Phys. Rev. Lett. **97**, 242003 (2006).
2. V. M. Abazovy et al., The D0 Collaboration, Phys. Rev. Lett. **98**, 181802, (2007), T. Aaltonen et al., The CDF Collaboration, Phys. Rev. Lett. 103, 092002 (2009).
3. V. M. Abazov, et al., The D0 Collaboration, Phys. Rev. Lett. 95, 141802 (2005), V. M. Abazov, et al., The D0 Collaboration, Phys. Rev. D 76, 111104 (2007), A. Abulencia *et al*, The CDF Collaboration, Phys. Rev. Lett. **98**, 161801 (2007).
4. A. Abulencia *et al*, The CDF Collaboration, Phys. Rev. Lett. 100, 201801 (2008), V. M. Abazov et al. The D0 Collaboration, Phys. Rev. Lett. 101, 171803 (2008)
5. V. M. Abazov et al. D0 Collaboration, Phys. Rev. Lett. 102, 161801 (2009), T. Aaltonen et al., The CDF Collaboration, arXiv:0911.4449, T. Aaltonen et al., The CDF Collaboration, arXiv:0905.4714
6. T. Aaltonen et al., The CDF Collaboration, Phys. Rev. Lett. **104**, 061803 (2010)
7. V. M. Abazov, et al., The D0 Collaboration, Phys. Rev. Lett. **104**, 061804 (2010)
8. T. Aaltonen et al., The CDF and D0 Collaborations, Phys. Rev. Lett. **104**, 061802 (2010)